OPEN ACCESS

University of Dundee

University of Dundee

Thermal behaviour of concrete sandwich panels incorporating phase change material

Sukontasukkul, Piti; Sangpet, Teerawat; Newlands, Moray; Tangchirapat, Weerachart; Limkatanyu, Suchart; Chindaprasirt, Prinya

Published in:
Advances in Building Energy Research

DOI:
10.1080/17512549.2020.1788990

Publication date:
2022

Document Version
Peer reviewed version

Link to publication in Discovery Research Portal

Citation for published version (APA):
Sukontasukkul, P., Sangpet, T., Newlands, M., Tangchirapat, W., Limkatanyu, S., & Chindaprasirt, P. (2022). Thermal behaviour of concrete sandwich panels incorporating phase change material. *Advances in Building Energy Research*, *16*(1), 64-88. https://doi.org/10.1080/17512549.2020.1788990

General rights
Copyright and moral rights for the publications made accessible in Discovery Research Portal are retained by the authors and/or other copyright owners and it is a condition of accessing publications that users recognise and abide by the legal requirements associated with these rights.

• Users may download and print one copy of any publication from Discovery Research Portal for the purpose of private study or research.
• You may not further distribute the material or use it for any profit-making activity or commercial gain.
• You may freely distribute the URL identifying the publication in the public portal.

Take down policy
If you believe that this document breaches copyright please contact us providing details, and we will remove access to the work immediately and investigate your claim.

Download date: 04. May. 2023

Thermal Behavior of Concrete Sandwich Panels Incorporating Phase Change Material

Piti Sukontasukkul[1*], Teerawat Sangpet[2], Moray Newlands[3], Weerachart Tangchirapat[4], Suchart Limkatanyu[5], Prinya Chindaprasirt[6]

[1]Professor and Corresponding Author, Construction and Building Materials Research Center, Department of Civil Engineering, King Mongkut's University of Technology North Bangkok, Thailand, Email: piti@kmutnb.ac.th; piti.s@eng.kmutnb.ac.th; piti.kmutnb@gmail.com

[2]Lecturer, Department of Mechanical and Aerospace Engineering, King Mongkut's University of Technology North Bangkok, Bangkok, Thailand, Email: teerawat.s@eng.kmutnb.ac.th

[3]Senior Lecturer, School of Science and Engineering, University of Dundee, UK, Email: m.d.z.newlands@dundee.ac.uk

[4]Associate Professor, Department of Civil Engineering, King Mongkut University of Technology Thonburi, Bangkok, Thailand, Email: weerachart.tan@kmutt.ac.th

Professor, Department of Civil Engineering, Faculty of Engineering, Prince of Songkla University, Songkla, Thailand, 90112, Email: suchart.l@psu.ac.th

[6]Professor, Sustainable Infrastructure Research and Development Center, Department of Civil Engineering, Khon Kaen University, Thailand, Email: prinya@kku.ac.th

Abstract

In this study, the influence of phase change materials (PCM) on the thermal behavior of concrete sandwich panels was investigated. Sandwich panels are known for their high thermal efficiency however, this research proposed the integration of a PCM concrete layer to maximize the ability of PCM to store heat and slow down the rate of heat transfer. The

This is an Accepted Manuscript of an article published by Taylor & Francis in *Advances in Building Energy Research* on 8 July 2020, available online: https://doi.org/10.1080/17512549.2020.1788990

thermal behavior was tested by supplying heat energy to specimens until the core temperature reached 60^{o}C. Specimens were allowed to cool until the core temperature returned to 40^{o}C. The thermal behavior was recorded and analyzed. Three specimen types were tested: solid panels (SL), sandwich panels (SW) with and without a PCM concrete layer. For all SW panels, a 10-mm air gap was introduced between two layers at three different locations. Results showed that the air gap behavior was modified with the heat transfer process by creating temperature lagging, thus resulting in a slower rate of heat transfer across the specimens. The temperature lagging was observed in SW panels and varied depending on location of the air gap. The application of PCM in SW panels further reduced the rate of heat transfer and decreased the fluctuation of temperature lagging magnitude.

Keywords: Concrete Sandwich Panel; Phase Change Materials; Thermal Behavior; Temperature Lagging; Rate of Heat Transfer

1. Introduction

Thermal comfort is one of several comforts factors required for humans to reside in a building. There are several approaches in the design and construction processes of a building that can achieve an optimal thermal comfort zone. Some examples include the use of architectural design to provide shades and openings, the use of landscape design to direct wind flow or sunlight (Yu & Hien 2009; Qiu et al. 2007), the use of materials with low thermal conductivity to slow down the rate of heat transfer (Ghosh et al. 2018; Sukontasukkul et al. 2019, O'Flaherty et al. 2019) or the use of air conditioning to adjust living temperature (Zhao et al. 2018; Zhao, Z., & Yu, N. 2017; Doiphode 2018). The former three approaches are considered passive thermal control while the latter one is considered active thermal control (Amirifard et al. 2019; Pisello et al. 2013).

While the choice of active thermal control appears more attractive due to its effectiveness and easy implementation, it has a disadvantage in terms of energy consumption. In cases where fossil fuels are used as source of energy, negative environmental impacts such as greenhouse gas emissions or natural resource depletion are inevitable. In some cases, passive thermal control may not be as effective as active thermal control, however, with correct design considerations, it is often more attractive in terms of environmental friendliness and whole life cost because, after installation, it requires only a small amount of energy to maintain. The effectiveness of the passive thermal control system, however, depends mainly on the system used and material selection (Berghout & Forgues 2019; Amirifard et al. 2019).

The use of sandwich panels is one of many passive systems known to have the potential to display high thermal efficiency (Alvez-Ramirez et al. 2012; Ng & Low 2010; Ng, Low, & Tioh 2011; Castellón et al. 2010). Typically, a sandwich panel consists of two elements: surface and core. The outer and inner surfaces are usually made of rigid, strong materials such as concrete, steel or metallic plates or timber, to provide load bearing capacity. The core, on the other hand, is made of lightweight or highly insulated materials such as porous concrete, foam, synthetic, or natural fibers.

There are a number of studies investigating the thermal efficiency of concrete sandwich panels with different core materials. Alavez-Ramirez et al. (2012) measured thermal conductivity of coconut fiber filled sandwich ferrocement panels. A thermal conductivity of 0.210 W/m.K was reported for coconut fiber filled sandwich ferrocement panels, which was lower than that of lightweight concrete brick (0.536), hollow core concrete brick (0.683), red clay brick, (0.930) and ferrocement panel (0.696). The thermal conductivity decreased with increasing coconut fiber content. Ng & Low (2010) and Ng, Low, & Tioh (2011) investigated

the thermal conductivity of sandwich panels with surfaces made of aerated lightweight concrete and a core made of newspaper. A reduction in thermal conductivity of 18-22% was reported when a newspaper core (intensity of 0.05 g/cm^2 (0.0005 g/mm^2)) was used. Castellón et al (2010) investigated the effect of microencapsulated PCM in sandwich metal sheet panels made of galvanized pre-lacquered steel. They reported an increase in thermal inertia when microencapsulated phase change material (PCM) was incorporated into the sandwich metal sheet.

On the material side, concrete itself is known have low thermal conductivity. To further improve the thermal properties, air voids can be incorporated into concrete mixture through porous aggregates or within the cement paste. However, the addition of air voids can cause a decrease in structural capacity. To avoid this, thermal enhancing agents such as PCMs can be used. Phase change materials are materials with high latent heat capable of changing phase at specific temperatures. In the process of changing phase, energy is stored in the PCM whilst it is in its liquid phase and released during PCM solidification process. These properties can be beneficial in improving thermal storage, slowing down the rate of heat transfer and modifying the time to reach peak temperatures within construction materials (Sharma, 2013; Abhat, 1983; Lorsch et al., 1976; Abhat, 1981; Rajagopal et al.2017; Muthuvelan et al. 2018).

One of the first documented uses of PCM being implemented as a part of housing envelopes to store solar heat is shown in Telkes, 1947. Since then, it has been widely used in various kinds of construction materials such as gypsum boards (Oliver, 2012; Shukla, Fallahi, & Kosny, 2012), masonry blocks (Silva et al., 2015; Vicente & Silva, 2014) or concrete (Cunha, Lima, & Aguiar, 2016; Sukontasukkul et al., 2018; Boh & Sumiga, 2008; Ling & Poon, 2013; Cao et al., 2017; Sakulich & Bentz, 2012; Sukontasukkul et al., 2016; Jayalath, 2016; Ramakrishnan, 015).

A recent study by the authors (Sukontasukkul et al., 2019) investigated the latent heat of concrete incorporating high contents (up to about 8% by total weight of concrete) of polyethylene glycol (PEG) within coarse aggregates. The latent heats of PCM concrete was found to increase from around 4,800 J/kg to 7,200 J/kg when conventional lightweight aggregates were replaced by PEG aggregates from 25% to 100% by volume.

This study aimed to further investigate the effect of high content PCM concrete by incorporating it into sandwich panel systems. Since the sandwich panel and PCM are both excellent in passive thermal control, the integration of PCM into the sandwich panel system should enhance the thermal properties of concrete even further. The experimental series included the investigation on thermal movement of sandwich panels compared to solid panels. Two types of sandwich panels, with and without a PCM layer, were prepared to investigate the effect of PCM on thermal behavior. A 10-mm air gap was inserted into sandwich panels at different locations to investigate location effect. The influence of PCM in terms of thermal movement, rate of heating and cooling down, and temperature lag were discussed.

2. Experimental Procedure

2.1. Materials

Materials used in this study consisted of Portland cement type I (ASTM C-150), fine aggregate (river sand), lightweight aggregate (LA), lightweight aggregate impregnated with phase change material (PCMLA) and a phase change material (PCM, paraffin 6035). Properties of the lightweight aggregates and PCM are given in Table 1 and Table 2.

2.2. Mix proportion

The mix proportions for normal lightweight concrete (NLC) was set at 1 : 0.42 : 1.40 : 1.02 (Cement : Water : Fine aggregate : Coarse aggregate) by weight. The regular lightweight concretes were used in the casting of NLC.

For PCM lightweight concrete (PCMLC), the entire volume of LA was replaced by PCMLA. The PCMLA were prepared by fully submerging oven-dried lightweight aggregates in a pan of liquid PCM at 120^{o}C and placing them in an oven at a temperature of 120^{o}C for 8 hours. As soon as the lightweight aggregates are submersed into the liquid PCM, the weight increased by approximately 7% due to self-sorptivity of the aggregates. After that the weight increased with time until reaching a steady state (stable). At the steady state, a maximum impregnation level of 15% by weight was achieved. This process gave the maximum PCM impregnation level of 15%, specific gravity (dry) of 1.3 and absorption of 0.2%. More details on the PCM impregnation process can also be found in Sukontasukkul et al, 2016.

The sandwich panel was designed to have dimensions of 400 x 400 mm with a total thickness of 100 mm. To investigate the effect of the air gap and its location, two types of panels were prepared: 1) solid (SL) and 2) sandwich panels (SW). The SL panels were cast with NLC for its full thickness (100 mm). The SW panels were prepared in three layers, consisting of two layers of NLC and one layer of a 10 mm air gap between the two NLC layers. The air gap location was varied from 30 mm, 45 mm, and 60 mm from the front surface as shown in Fig. 1.

To investigate the effect of PCMLC and its location, P-N panels with a front layer made of PCMLC and a back layer made of NLC were prepared. A 10mm air gap was inserted at two different locations from the front layer (30 mm and 60 mm) (Fig. 1).

Actual pictures of the specimens are given in Fig. 1. Each specimen was held together by 4 plastic spacers at the corners. Each spacer did not only hold the specimen in place but also provided air gap of 10 mm at the specified location.

Details of each panel type are summarized in Table 3.

2.3. Experimental Series

Two experimental series were carried out. The first was to measure general properties of both NLC and PCMLC concrete, such as unit weight and absorption (ASTM C138), abrasion (ASTM C779), flexural (ASTM C78) and compressive strengths (EN12390).

The abrasion test was carried out based on ASTM C779 Procedure B. Testing equipment consists of a motor-driven spider arrangement that rotates at 56 revolutions per minute, suspended from the motor shaft. The three shafts were fitted with a yoke inside, upon which a series of seven dressing wheels were placed on a horizontal axle. The mass of each complete dressing wheel was 7.5 kg. The measuring instrument was a digital micrometer indicator with reading accuracy of 0.001 mm, range of 12.7 mm (0.5 in.) and working temperature of 0-40^{o}C. The universal testing machine (Instron 8850) with 1500 kN axial load capacity was used in testing for flexural and compressive strength of concrete.

The second series was to investigate the thermal behavior of the panels. The test was carried out using the 800 x 800 x 2000 mm heat insulating chamber constructed at KMUTNB (Fig. 2). The chamber was equipped with a 1500 W spotlight (heat source) and an insulated partition with specimen supporter (Fig. 1). Prior to the test, three or four (depending on the specimen setup) thermocouples were installed on the specimen on locations as shown in Fig. 3. The

thermocouples used were type T with duplex insulation, capable of measuring temperatures from -200/+350°C with a special limit of errors of ±0.4% in accordance to ANSI.

For a solid panel, three thermocouples were placed at the front (F_{sl}), center (C_{sl}), and back (B_{sl}) surface of the specimen. For a sandwich panel, thermocouples were placed on the specimen in four locations: one at the front (F_{sw}), two at the air gap location (one on back surfaces of the first concrete layer (C_{sw1}), one at the front surface of the second concrete layer (C_{sw2})), and the last one at the back surface of the panel (B_{sw}).

After a specimen was secured on the specimen supporter, the test started by supplying heat to the specimen until the temperature at the 2nd thermocouple of the panel reached 60°C (location C_{SL} for SL panel and C_{SW1} for SW panel), after which the heating stopped. The temperature of 60°C was selected based on the PCM melting temperature to ensure that the PCM of the entire front portion of SL panel or the front layer of SW panel was fully melted.

After the heating process stopped, the specimen was allowed to cool down until the temperature was about 40°C, then the test was terminated. Data on thermal behavior was collected using an automatic data acquisition system.

3. Results and Discussion

3.1. Concrete Properties

The properties of NLC and PCMLC are shown in Table 4. The PCMLC exhibited higher density than the NLC primarily due to PCM aggregates having a higher density than the normal aggregates. Higher density also implied that PCMLC was less porous than NLC, causing the absorption to decrease by 15.8%, and compressive and flexural strengths to increase by 56.1 % and 12.9% respectively. Sukontasukkul et al. (2019) reported the increased in both

compressive and flexural strengths in concrete mixed with aggregates impregnated with polyethylene glycol. The decrease in weight loss due to abrasion testing was 61% and was attributed to the improvement in strengths of PCMLC comparing to NLC and better abrasion resistance of PCM aggregates.

3.2. Thermal Behavior Concrete Sandwich Panel Systems

3.2.1. Influence of Air Gap: Solid vs. Sandwich Panels

To investigate the effect of the air gap on the thermal behavior of concrete panels, the sandwich panel with an air gap located at the center (N-N (4.5-1.4.5)) was used in comparison to the solid panel (N10). The temperature profiles along the panel's thickness on heating up and cooling down processes are shown in Fig. 4 and 5, respectively.

3.2.1.1. Temperature Profiles: Heating Cycle

For the solid panel, the temperature profiles measured at 1200, 2400 and 3600 seconds (20, 40 and 60 minutes) showed a smooth trend line from front to back surface (Fig. 4). The temperature was highest at the front and lowest at the back surface. In the case of the sandwich panel, the typical temperature profile was not a smooth trend line and conversely, temperature lagging was observed at the air gap location. The presence of an air gap caused heat to dissipate to the surrounding air, interrupting the continuous heat transfer along the thickness and causing the temperature of back layer to increase at slower rate (maintained temperature level). Similar study on the effect of air gap by Liu et al. (2018) showed that the addition of a hollow air gap between the inner and outer walls can reduce the temperature of the outer wall and improve the insulation effect. With the increasing air gap thickness, the thermal insulation effect was improved due to the increase of the thermal convection of the air.

By setting the initial temperatures of 25°C for both panel types, the rate of temperature heating up (surface heat up rate) from 25°C at different locations was calculated using Eq. 1 and the results are given in Table 5.

$$\dot{T}_{heat} = \frac{(T_t - T_{ini})}{t} \quad (1)$$

where $\dot{T}_{heat}$ is the surface heat up rate (°C/minute), T_t is the temperature at any time t (°C), Ti_{ni} is the initial temperature (°C), and t is time (minutes).

At the front surface (F_{sl} and F_{sw} locations), the temperature was found to increase at similar rates, with average values between 1.27 to 2.35 °C/min for both solid and sandwich panels. The $\dot{T}_{heat}$ was found to decrease with time from 2.35 °C/min at 1200 sec to 1.27 °C/min at 3600 sec. The reduction in the $\dot{T}_{heat}$ with time was due to the increasing heat conduction through the thickness of the specimen. As the temperature increased, the temperature difference between front and back surface increased gradually. This caused the heat to conduct more to the back and also slowed down the $\dot{T}_{heat}$ at the front location.

The center location is where the air gap effectively influences the heat transfer. For the solid panel, the $\dot{T}_{heat}$ at the center location (C_{sl}) is observed around 0.59-0.66 °C/min. In case of sandwich panel, the temperature changes were measured at two locations (C_{sw1} and C_{sw2}). The C_{sw1} location was measured at the back surface of the front concrete layer and the $\dot{T}_{heat}$ was observed around 0.44-0.51 °C/min, which was about 16 to 40% lower than those of solid panels. This is perhaps due to the effect of the air gap, which allowed heat to dissipate through the surrounding air.

At the location C_{sw2} which is 10 mm across the air gap (front surface of the second concrete layer), a similar effect to that of C_{SW1} took place. The existence of air gap interrupted the heat

conduction process and heat was transferred through air instead of the solid (convection). Since the convection process is generally slower than conduction, this led to a reduction of $\dot{T}_{heat}$ at C_{SW2} by 143 to 413% to around 0.08 to 0.12 ^{o}C/min.

At the back location, since the heat transfer of the sandwich panels was interrupted by an air gap, the heat up rates of the sandwich panel were found to be much lower than those of solid panel by 2 to 3 times. The heat up rate of the solid and sandwich panels were observed around 0.19-0.36 ^{o}C/min and 0.08 to 0.12 ^{o}C/min, respectively (Table 5). The heat up rate at the back surface was found to increase with time. The reason or this contrary behavior was due to the fact that at the beginning the temperature of both sides were almost similar, the rate of heat transfer was low, however, with rapid increase of temperature at the front surface, the temperature difference began to increase and heat was transferring to the back surface at faster rate causing the heat up rate of the back surface to increase with time.

3.2.1.2. Temperature Profile: Cooling Cycle

Figure 5 shows the temperature profiles of both solid and sandwich panels in the cooling down process. Observation showed the SL panel exhibited a smooth and (almost) linear temperature gradient curve and the heat transfer appeared uninterrupted throughout the entire thickness. The SW panel, on the other hand, exhibited a drop in the temperature gradient curve, with an interruption at the location of air gap. The effect of the air gap also influenced the rate of temperature cool down in SW panels.

In order to calculate the cool down rate, the reference final temperature (Tf) was set at 40^{o}C at the front location of both panel types. Using temperature at end of heating cycle and time require to cool down from the end of heating cycle to 40^{o}C, the rate of cool down can be calculated by Eq. 2 and results are shown in Table 5.

$$\dot{T}_{cool} = \frac{(T_h - T_f)}{\Delta t} \quad (2)$$

where $\dot{T}_{cool}$ is the surface temperature cooling down rate (°C/minute), T_h is the temperature at the end of heating cycle (°C), T_f is the final temperature (°C), and Δt is time required to reach final temperature (minute).

Based on the thermal behavior exhibited in Fig. 4 and results shown in Table 5, the SL panel tended to cool down faster than the SW panel. At the front layer, the rates of temperature cool down of SL and SW panels ranged from 0.15 to 0.24°C/min and from 0.11 to 0.17°C/min, respectively. The SW was cooling down slower than the SL panel by about 30-40%. The cooling down rate was found to decrease gradually with time due to the decreasing temperature difference as the specimen cooled down.

The cooling down rate at the center location was also observed to be faster in the SL panel than in SW panel by about 45-63%. At the air gap location, the temperature difference between C_{SW1} and C_{SW2} was large at the beginning of the cool down process but decreased with time.

On the back surface, similar to the front and center, the cool down rate of SL panel was faster than SW panel by about 5 to 13 times. Also, for SL panel, the cooling down rate was found to decrease with time due to the decrease in temperature difference between front and back locations. However, for SW panel, the cooling down rate at the B_{SW} location was found to increase with time. This was mainly because of the heat trapped in the air gap. From Fig. 5, the observation of temperature lag indicated that heat was actually trapped at this location and the nearly constant temperature the C_{SW2} location also provided a clear evidence that heat at this location remained unchanged. As time passed, the temperature difference

between C_{SW2} and B_{SW} remained large while the temperature of the surrounding reduced significantly. This caused the heat transfer rate to increase in order to enter the balance.

3.2.2. Temperature Profile: Effect of Air Gap Location

This section discussed the effect of air gap location on thermal behavior of sandwich panels. A 10 mm air gap was inserted in the middle of the panel at three different locations: 30 mm, 45 mm, and 60 mm as shown in Fig. 1.

In general, all sandwich panels exhibited similar unsmooth curves with temperature lagging due to the effect of air gap ("*fib* Bulletin No. 84," 2017). Thermal behavior on both heating up and cooling down processes are shown in Fig. 6.

On heating up, at 1200 seconds, the temperatures at the front surface of all panel types were more or less the same (Fig.6a). With increasing time, the temperature increased faster in panels with thinner front layer. At 2400 seconds, the outside temperature of the N-N(3-1-6) panel was the highest among the three panel types, followed by N-N(4.5-1-4.5) and N-N(6-1-3). At 3600 seconds, the N-N(3-1-6) had already reached the peak temperature and had started the cooling down process while the N-N(4.5-1-4.5) and N-N(6-1-3) had not reached peak temperature yet and were still in the process of heating up (Fig.6c). At 4800 seconds, the N-N(4.5-1-4.5) had passed the peak temperature and was in the cool down process, similar to N-N(3-1-6) (Fig.6d).

On the cool down process, at 6000s, the N-N(6-1-3) which had the thickest front layer had just reached the peak temperature and all panels underwent the cool down process (Fig. 6e). At 12000 seconds, all panels were cooling down for quite some time, the panels with thicker front layer appeared to have inside residual temperatures higher than those with thinner

front layers. This is partly because the N-N(6-1-3) took longer to heat up to the peak, so it had been subjected to heat for longer period of time. Also, panels with a thinner front layer took less time to dissipate heat out to the outside atmosphere than those with a thicker front layer.

The temperature lag (or the temperature difference at C_{SW1} and C_{SW2} location) for N-N(3-1-6) and N-N(6-1-3) panels were plotted against time as shown in Fig. 7. Typically, the temperature lagging increased gradually with time during the heat up process, reached the maximum around the time when the peak temperature was reached, and then decreased gradually in the cool down process. Both panels exhibited different temperature lag at different times. The N-N(3-1-6) panel was found to have maximum lag of about 20.9^{o}C at 3000 seconds while the N-N(6-1-3) was found to have a lag of 16.2^{o}C at 6000 seconds.

Larger temperature lag in SW panels with a thinner front layer was the direct result of the faster increase in temperature of panel with thinner thickness. In thinner panels, the temperature at both front and back surface can be driven faster than thicker panels. As the heat was supplied to the panel, the temperature of the front layer of panels with a thinner front increased quicker than those with a thicker front layer. This caused the temperature in the front layer (at F_{SW} and C_{SW1} locations) to increase quickly, while the temperature at the back layer (C_{SW2}) was not being accelerated at the same rate due to the effect of energy dissipating at the air gap. As the heating time increased, temperature difference (temperature lag) between the C_{SW1} and C_{SW2} locations kept spreading out and reached maximum at the peak temperature (60^{o}C). Thus, because of its thinner front layer, the temperature lag of N-N(3-1-6) panel was found to be larger than that of N-N(6-1-3).

3.2.3. Influence of PCM Layer (N-N vs. P-N)

In this phase of the study, the NLC layer at the front layer was replaced by a PCMLC layer in two panel types (3-1-6 and 6-1-3) and then subjected to a similar process of thermal testing. Results are shown in Fig. 8 and 9.

3.2.3.1. Temperature Profile: Heating Cycle

For both panel types, the panels with front layer made of PCM concrete was found to heat up slower than those made of normal concrete (Fig.8). Before any part of the front layer reached 60°C, the temperatures of both N-N and P-N panels were found to increase at the same rate. As soon as any portion of P-N panel reached 60°C, the PCM in that portion began to change phase from solid to liquid and stored energy simultaneously (Ling & Poon, 2013; Newell, P. & Xi, Y., 2012). This caused the heat up to slow down in that portion. As heat advanced further, the phase changing process took place deeper into the thickness and more energy was stored. The energy storage was assumed to stop when PCM of the entire front layer melted or the temperature of the entire front layer reached 60°C or higher.

Table 6 shows the time required to drive the temperature at C_{SW1} location to 60°C. Assuming that temperature increased at a constant rate, the rate of heat up per minute of the front layer can be calculated using Eq.1. In general, for both panel types, the average rate of temperature heating up of the front layer was faster in the thinner panel (3-1-6) than the thicker panel (6-1-3). Comparing between N-N and P-N, the effect of PCM delaying the heat up process can be seen by the longer duration required to heat up to 60°C. With a similar target temperature, a longer time implied that heat was traveling at slower rate. The P-N panels exhibited a 20% to 47% lower rate of heating up compared to N-N panels with similar configuration.

3.2.3.2. Temperature Profile: Cooling Cycle

The cool down process began when the supply of heat was ceased. Since the 3-1-6 panel was heated more quickly than the 6-1-3 panel, the cool-down process began earlier. In addition, because of its thinner front layer, the rate of cool-down was also faster.

Comparing N-N and P-N panel types, the P-N panels tended to cool down slower than the N-N panels (Fig.9). This contributed mainly to the effect of PCM changing phase back from liquid to solid which, in the process, released the stored energy back to the system. The solidification process began in the portion with a temperature lower than 60^{o}C, where PCM began to solidify and released energy back into the system. The released energy caused the temperature to remain stable for a period of time and slowed the rate of cooling down. Similar to the liquidation process, the solidification advanced deeper into the section with cooling time and stopped when the entire section had a temperature lower than 57^{o}C.

3.2.3.3. Temperature lag at the air gap

Different characteristics of temperature lag can be used to identify the effect of PCM on the thermal behavior of SW panels. The temperature lag at the air gaps was calculated by subtracting temperature at the back surface of the front layer (C_{SW1}) with the temperature at the front surface of the back layer (C_{SW2}) and the results are given in Fig. 10 and Fig. 11.

As discussed previously in Section 3.2.2, the temperature lag increased with the heat-up time, reached its maximum lagging at peak temperature, and then decreased with cool-down time. SW panels with thin front layers exhibited faster and larger lagging than those with thick front layers. A similar observation was also found in P-N panels. The P-N(3-1-6) exhibited larger maximum lag and faster time to reach peak temperature than the P-N(6-1-3) by 34% and 81%, respectively.

Comparing between N-N and P-N panels, regardless of panel type, the existence of PCM helped slow down the time to reach peak temperature and reduced the level of maximum temperature lagging. For both panel types, the maximum lag of P-N panels was smaller than that of N-N panels by 20% to 24%. For N-N panels, as soon as the heating began, the temperature of the front layer was driven up quickly and reached peak in a short period of time. Since the temperature at C_{SW1} reached peak after a very short period of time, the temperature at C_{SW2} had not increased at that point. This phenomenon created a larger temperature lag between C_{SW1} and C_{SW2} locations.

On the other hand, for P-N panels, the effect of PCM phase changing and energy storage slowed down the rate of heat transfer. This allowed the temperature to increase slowly and reach its peak after a longer period of time. In addition, by the time that the temperature at C_{SW1} location reached its peak (at 60°C), the temperature at C_{SW2} location began to rise as well. This phenomenon caused the temperature lag to be smaller and temperature levels across the panel to be more stable.

3.2.4. Decrement factor

The decrement factor refers to the amount by which conditions are moderated by an element of a building. In the case of the peak temperature on the outer surface of a building on a summer day, this would be the amount by which the peak is reduced by the time it reaches the inner surface. It can be calculated Eq.3 and results are shown in Fig. 12.

$$Decrement\ factor = \frac{T_{max}^{in}}{T_{max}^{out}} \quad (3)$$

where T_{max}^{in} is the maximum inside temperature and T_{max}^{out} is the maximum outside temperature.

For plain concrete, the decrement factor was calculated as 0.487, 0.384, 0.379 and 0.347 for N(10), N-N(6-1-3), N-N(4.5-1-4.5) and N-N(3-1-6), respectively. The solid panel N(10) exhibited the highest decrement factor of 0.487. The decrement factor was found to be lower in the sandwich panels due to the effect of air gap incorporated into the wall system. When PCM concrete was used in the sandwich panel, the decrement factor reduced to 0.367 and 0.333 for P-N(6-1-3) and P-N (3-1-6), respectively. In this case, the effect of PCM played a role in delaying the time and caused the peak temperature at the back surface to decrease.

Similar results were previously reported by Udawattha & Halwatura (2018) who investigated time lag and decrement factor of concrete blocks. They reported a time lag of about 1 to 3 hours and a decrement factor of 0.962 to 0.978 depending on type of concrete blocks. Ramin et al (2016) studied effect of insulation thickness and wall orientation on decrement factor of houses in Iran. The decrement factor was found to decrease with the increasing insulation thickness with walls facing east also yielding the lowest decrement factor. Naouel et al. (2010) also reported the time lag up to 7 hours in the thermal analysis of insulated walls.

3.2.5. Thermal Gradient and Percentage Dissatisfied

The analysis on this phase of the study was carried out based on ISO 7730: Ergonomics of the thermal environment - Analytical determination and interpretation of thermal comfort using calculation of the Predicted Mean Vote (PMV) and Predicted Percentage Dissatisfied (PPD) indices and local thermal comfort criteria, to investigate the effect of thermal gradient of thermal discomfort in form of percentage dissatisfied (PD). The following equations were used in accessing percentage dissatisfy in 2 categories: cold and warm walls.

Cold wall: $PD = \frac{100}{1+EXP(6.61-0.345\Delta t_{pr})}$ for $\Delta t_{pr} < 15^{o}C$ (4)

Warm wall: $PD = \frac{100}{1+EXP(3.72-0.052\Delta t_{pr})} - 3.5$ for $\Delta t_{pr} < 35^{o}C$ (5)

where PD is the percentage dissatisfied (%) and Δt_{pr} is the radiant asymmetry (^{o}C).

Using test results, the percentage dissatisfied of plain concrete and PCM concrete sandwich panels are plotted in Fig. 13. The curves provide a conservative estimate of the discomfort: no other positions of the body in relation to the surfaces (e.g. front/back) cause higher asymmetry discomfort. In the case of plain concrete sandwich panel, the maximum PD for cold and warm walls were 7.36% and 16.03%, respectively. When PCM concrete was incorporated into the panel (as the front layer of sandwich panel system), the maximum PD for both cold and warm walls were 6.54% and 13.73%, respectively. This indicated that the effect of the PCM layer in the sandwich panel system can help reduce the thermal discomfort as seen by the reduction in PD values.

4. Conclusions

Based on the obtained results, the following conclusions can be drawn:

- From a comparison between solid and sandwich panels, the effect of introducing an air gap was significant in interrupting the heat transfer process through the panel and caused the mode of transfer to change from conduction (through solid medium) to convection (through air) instead. This slowed down the heat-up rate of the back layer and kept the temperature of sandwich panels lower than the solid panels.
- On the effect of air gap location, temperature increase was more noticeable when an air gap was placed closer to the front surface because the front layer was thinner. As the air gap moved deeper (further from the heat source), the front layer became

thicker and the heat-up rate then reduced. The temperature lagging effect also increased when the air gap was closer to the front surface (closer to the heat source) and decreased as the air gap moved towards the back surface.

- The presence of PCM concrete in the front layer helped to reduce the heat up rate even further. A comparison between N-N and P-N panels showed the heat up rate decreased by up to 47% mainly due to the effect of latent heat storage during the phase changing transition. The phase transition also affected the temperature behavior during the cool-down process and allowed the heat remain stored in the panels for longer period of time. The temperature lag was also found to be lower in P-N than N-N panels by up to 24%.
- Based on ISO 7730, the use of PCM concrete in sandwich panel system help reduce thermal discomfort as seen by the decreasing value of percentage dissatisfied. However, this conclusion is based on local discomfort in the case of radiant asymmetry, it cannot be applied to overall discomfort of the whole system which will require further and in-depth analysis.

5. Acknowledgement

This research was funded by King Mongkut's University of Technology North Bangkok under contract no. KMUTNB-63-KNOW-024. The 5th author (Suchart Limkatanyu) would like to acknowledge funding from TRF Senior Research Scholar (RTA 6280012). Special thanks are also due to the senior students involved in this project.

6. Conflict of Interest

The authors declare no conflict of interest.

7. References

[1] Abhat, A. (1983). Low temperature latent heat thermal energy storage, Heat storage materials. Solar Energy, 30, 313–332.

[2] Abhat, A., Heine, D, Heinisch, M, A. Malatidis, N, & Neuer, G. (1981). Development of a modular heat exchanger with an integrated latent heat storage (report no. BMFT FBT 81-050). Stuttgart, Germany: Germany Ministry of Science and Technology Bonn

[3] Alavez-Ramirez, R., Chiñas-Castillo, F., Morales-Dominguez, V.J., & Ortiz-Guzman, M. (2012). Thermal conductivity of coconut fibre filled ferrocement sandwich panels. Construction and Building Materials, 37, 425-431.

[4] Amirifard, F., Sharif, A.M., & Nasiri, F. (2019). Application of passive measures for energy conservation in buildings – a review, Advances in Building Energy Research, 13:2, 282-315, DOI: 10.1080/17512549.2018.1488617.

[5] ASTM International (2019). ASTM C138 / C138M - 17a: Standard Test Method for Density (Unit Weight), Yield, and Air Content (Gravimetric) of Concrete, West Conshohocken, PA, USA.

[6] ASTM International (2016). ASTM C779/C779M-19: Standard Test Method for Abrasion Resistance of Horizontal Concrete Surfaces, West Conshohocken, PA, USA.

[7] ASTM International (2018). ASTM C78/C78M-18: Standard Test Method for Flexural Strength of Concrete (Using Simple Beam with Third-Point Loading), West Conshohocken, PA, USA.

[8] Berghout, B., & Forgues, D. (2019). Passive ambient comfort and the interaction of vernacular strategies and devices in arid zone habitat design: case of Biskra, Algeria, Advances in Building Energy Research, DOI: 10.1080/17512549.2019.1607775

[9] Boh B., & Sumiga B. (2008). Microencapsulation technology and its applications in building construction materials. RMZ—Materials and Geoenvironment, 55 (3), 329–44.

[10] Castellón, C., Medrano, M., Roca, J., Cabeza, L.F., Navarro, M.E., Fernández, A.I., Lázaro, A., Zalba, B. (2010). Effect of microencapsulated phase change material in sandwich panels. Renewable Energy, 35(10), 2370-2374

[11] Cao V.H., Pilehvar S., Salas-Bringas C., Szczotok A.M., Rodriguez J.F., Carmona M., Nodar Al-Manasir, & Kjøniksen A. (2017). Microencapsulated phase change materials for enhancing the thermal performance of Portland cement concrete and geopolymer concrete for passive building applications. Energy Conversion and Management, 133, 56-66.

[12] Cunha S., Lima M., & Aguiar J.(2016). Influence of adding phase change materials on the physical and mechanical properties of cement mortars. Construction and Building Materials, 127, 1-10.

[13] Doiphode, P., Jadhav, A., Kumar, M., & Samanta, I. (2018). Thermo-flow performance analysis of split air conditioner under high-speed winds around buildings, Advances in Building Energy Research, DOI: 10.1080/17512549.2018.1520644

[14] Fédération internationale du béton. (2017), *fib* Bulletin No. 84: Precast Insulated Sandwich Panels- State of the art report, ISSN. 978-2-88394-124-3.

[15] Ghosh, A., Ghosh, A., & Neogi, S. (2018). Evaluation of physical and thermal properties of coal combustion residue blended concrete for energy efficient building application in India, Advances in Building Energy Research, DOI: 10.1080/17512549.2018.1557076

[16] International Organization for Standardization (2005). ISO 7730:2005 – Ergonomics of the thermal environment — Analytical determination and interpretation of thermal comfort using calculation of the PMV and PPD indices and local thermal comfort criteria, Switzerland.

[17] Jayalath, A., Nicolas, R.S., Sofi, M., Shanks, R., Ngo, T., Aye, L., & Mendis, P. (2016). Properties of cementitious mortar and concrete containing micro-encapsulated phase change materials. Construction and Building Materials, 120, 408-417.

[18] Ling T-C, & Poon C-S (2013). Use of phase change materials for thermal energy storage in concrete: An overview. Construction and Building Materials, 46, 55-62.

[19] Lorsch, H.G., Kauffman, K.W., & Denton, J.C. (1976). Thermal energy storage for heating and air conditioning, future energy production system. Heat Mass Transfer Proc., 1, 69–85.

[20] Liu, Y.J., Shen, M.G., Lv, Z.Q. & Han, X.H. (2018). Study on insulation effect of hollow riser. Metalurgija, 57, 146-148.

[21] Muthuvelan, T., Panchabikesan, K., Munisamy, R., Nibhanupudi K.M., & Ramalingam, V., (2018) Experimental investigation of free cooling using phase change material-filled air heat exchanger for energy efficiency in buildings, Advances in Building Energy Research, 12:2, 139-149, DOI: 10.1080/17512549.2016.1248487.

[22] Newell, P. & Xi, Y. (2012). Effect of Phase-Change Materials on Properties of Concrete. ACI Materials Journal, 109, 71-80.

[23] Ng, S.C., & Low, K.S., (2010). Thermal conductivity of newspaper sandwiched aerated lightweight concrete panel. Energy and Buildings, 42 (12), 2452-2456.

[24] Ng, S.C., Low, K.S., & Tioh, N.H. (2011). Newspaper sandwiched aerated lightweight concrete wall panels—Thermal inertia, transient thermal behavior and surface temperature prediction. Energy and Buildings, 43(7), 1636-1645.

[25] O'Flaherty, F.J., Khalaf F.J., & Starinieri V. (2019). Influence of nanomaterials on properties of lime and hemp/lime composites for energy efficient wall design, Advances in Building Energy Research, DOI: 10.1080/17512549.2019.1586584

[26] Oliver A. (2012). Thermal characterization of gypsum boards with PCM included: Thermal energy storage in buildings through latent heat. Energy and Buildings, 48, 1-7.

[27] Pisello, A.L., Santamouris, M., & Cotana F. (2013). Active cool roof effect: impact of cool roofs on cooling system efficiency, Advances in Building Energy Research, 7:2, 209-221, DOI: 10.1080/17512549.2013.865560

[28] Qiu, K., Haghighat, F., & Guarracino G. (2007). Thermal Behaviour of the Diffusive Building Envelope: State-of-the-Art Review, Advances in Building Energy Research, 1:1, 213-226, DOI: 10.1080/17512549.2007.9687276.

[29] Rajagopal, M., Babu, R.D., Antony Aroul Raj, V., & Velraj, R. (2017). Investigation on phase change material-based flat plate heat exchanger modules for free cooling applications in energy-efficient buildings, Advances in Building Energy Research, 11:2, 282-304, DOI: 10.1080/17512549.2016.1237379.

[30] Ramakrishnan, S., Sanjayan, J., Wang, X., Alam, M., & Wilson, J. (2015). A novel paraffin/expanded perlite composite phase change material for prevention of PCM leakage in cementitious composites. Applied Energy, 157, 85-94.

[31] Ramin, H., Hanafizadeh, P., & Akhavan-Behabadi M.A. (2016). Determination of optimum insulation thickness in different wall orientations and locations in Iran. Advances in Building Energy Research, 10:2, 149-171, DOI: 10.1080/17512549.2015.1079239

[32] Sakulich, A. R., & Bentz, D. P. (2012). Incorporation of phase change materials in cementitious systems via fine lightweight aggregate. Construction and Building Materials, 35, 483-490.

[33] Sharma, S.K. (2013). Zero energy building envelope components: a review. International Journal of Engineering Research and Applications, 3 (2), 662–675.

[34] Shukla, N., Fallahi, A., & Kosny, J. (2012). Performance characterization of PCM impregnated gypsum board for building applications. Energy Procedia, 30, 370-379.

[35] Silva T., Vicente R., Rodrigues F., Samagaio A., & Cardoso C. (2015). Performance of a window shutter with phase change material under summer Mediterranean climate conditions. Applied Thermal Engineering 84, 246-256.

[36] Sukontasukkul P., Sutthiphasilp T., Chalodhorn W. & Chindaprasirt P. (2018). Improving thermal properties of exterior plastering mortars with phase change materials with different melting temperatures: paraffin and polyethylene glycol. Advances in Building Energy Research, 2, 220-240.

[37] Sukontasukkul, P., Intawong, E., Preemanoch, P. Chindaprasirt, P. (2016). Use of paraffin impregnated lightweight aggregates to improve thermal properties of concrete panels. Materials and Structures 49, 1793.

[38] Sukontasukkul, P., Uthaichotirat, P., Sangpet, T., Sisomphon, K., Newlands, M., Siripanichgorn, A., Chindaprasirt, P. (2019). Thermal properties of lightweight concrete incorporating high contents of phase change materials. Construction and Building Materials, 207, 431-439.

[39] Telkes M. (1947). Solar house heating—a problem of heat storage. Journal Heat Ventilating, 44 (1947): 68–75.

[40] The British Standards Institution (2019). BS EN 12390-3:2019 - Testing hardened concrete. Compressive strength of test specimens, London, UK.

[41] Udawattha, C., and Halwatura, R., (2018). Thermal performance and structural cooling analysis of brick, cement block, and mud concrete block. Advances in Building Energy Research, 12:2, 150-163, DOI: 10.1080/17512549.2016.1257438

[42] Vicente, R. & Silva, T. (2014). Brick masonry walls with PCM macrocapsules: An experimental approach. Applied Thermal Engineering, 67, 24–34.

[43] Yu, C. & Hien W.N., (2009). Thermal Impact of Strategic Landscaping in Cities: A Review, Advances in Building Energy Research, 3:1, 237-260, DOI: 10.3763/aber.2009.0309

[44] Zhao, Z., Zhang, J., Cheng, H., & Shen, R. (2018). Numerical research on the operation characteristics of marine variable air volume air conditioning system, Advances in Building Energy Research, 12:2, 235-249, DOI: 10.1080/17512549.2017.1287128

[45] Zhao, Z., & Yu, N. (2017). The application of advanced control technologies in air conditioning system – a review, Advances in Building Energy Research, 11:1, 52-66, DOI: 10.1080/17512549.2015.1123650

Table 1 Properties of LA and PCMLA

Specification	Unit	LA	PCMLA
Maximum particle size	mm	10	10
Bulk Density	kg/m^3	645	890
Bulk specific gravity (Dry Basis)		1.08	1.300
Bulk specific gravity (SSD Basis)		1.25	1.303
Apparent specific gravity		1.30	1.304
Percent absorption	%	17.5	0.2
Weight loss (LA abrasion test)	%	31.7	12.1

Table 2 Properties of PCM used in study: Paraffin 6035

Specification	Unit	Value
Melting Point	°C	57.2-59.9
Specific Gravity	at 25 °C	0.89
Latent Heat	kJ/kg	189
Thermal Conductivity	W/m K.	0.21
Specific Heat	J/kg.K	2100
Oil Content	mass%	0.4
Penetration	at 25 °C	10.0-17.0
Color		30
UV Absorption		1.3

Table 3 Specimen configuration

Type	Solid Panel		Sandwich Panels				
	Mat.	Thick (mm)	Front layer		Air gap	Back layer	
			Mat.	Thick (mm)	Thick (mm)	Mat.	Thick (mm)
N10	NLC	100					
N-N (3-1-6)	-	-	NLC	30	10	NLC	60
N-N (4.5-1-4.5)	-	-	NLC	45	10	NLC	45
N-N (6-1-3)	-	-	NLC	60	10	NLC	30
P-N (3-1-6)	-	-	PCMLC	30	10	NLC	60
P-N (6-1-3)	-	-	PCMLC	60	10	NLC	30

Table 4 Properties of NLC and PCMLC aggregates

Property	**Unit**	**NLC**	**PCMLC**
Density	kg/m^3	1,747	1,873
Absorption	%	2.2	1.9
Weight loss (abrasion)	g	3.5	2.2
Compressive strength	MPa	18.7	29.2
Flexural strength	MPa	2.8	3.1

Table 5 Effect of air gap on rate of heating up and cooling down different location and time

Time, seconds	Front location		Middle location			Back location	
	N (10)	N-N (4.5-1-4.5)	N (10)	N-N (4.5-1-4.5)		N (10)	N-N (4.5-1-4.5)
	F_{SL}	F_{SW}	C_{SL}	C_{SW1}	C_{SW2}	B_{SL}	B_{SW}
Rate of Temperature Heating Up from 25°C ($\dot{T}_{heat}$)							
1,200	2.33	2.38	0.61	0.39	0.12	0.19	0.08
1,800	1.92	1.97	0.66	0.47	0.17	0.29	0.09
2,400	1.61	1.66	0.64	0.50	0.20	0.32	0.10
3,000	1.41	1.45	0.62	0.52	0.23	0.35	0.11
3,600	1.25	1.29	0.59	0.51	0.24	0.36	0.12
Rate of Surface Temperature Cooling Down to 40°C ($\dot{T}_{cool}$)							
6,000	0.24	0.17	0.19	0.12	0.048	0.14	0.011
6,600	0.21	0.15	0.18	0.11	0.049	0.14	0.013
7,200	0.19	0.15	0.16	0.11	0.051	0.13	0.015
7,800	0.18	0.13	0.16	0.10	0.051	0.13	0.016
8,400	0.17	0.13	0.15	0.10	0.052	0.13	0.017
9,000	0.16	0.12	0.14	0.09	0.052	0.11	0.019
9,600	0.15	0.11	0.13	0.09	0.053	0.11	0.020

Table 6 Rate of Temperature Heating Up of the Front Layer

Panel type	Heating up from 25°C		
	Duration, $t_t = t_{60}$ (second)	Peak temp, $T_t = T_{60}$ (°C)	Rate of heating up (°C/minute)
N-N (3-1-6)	3,213	59.5	1.11
P-N (3-1-6)	4,347	59.8	0.82
N-N(6-1-3)	6,552	60.5	0.55
P-N(6-1-3)	7,875	60.3	0.46

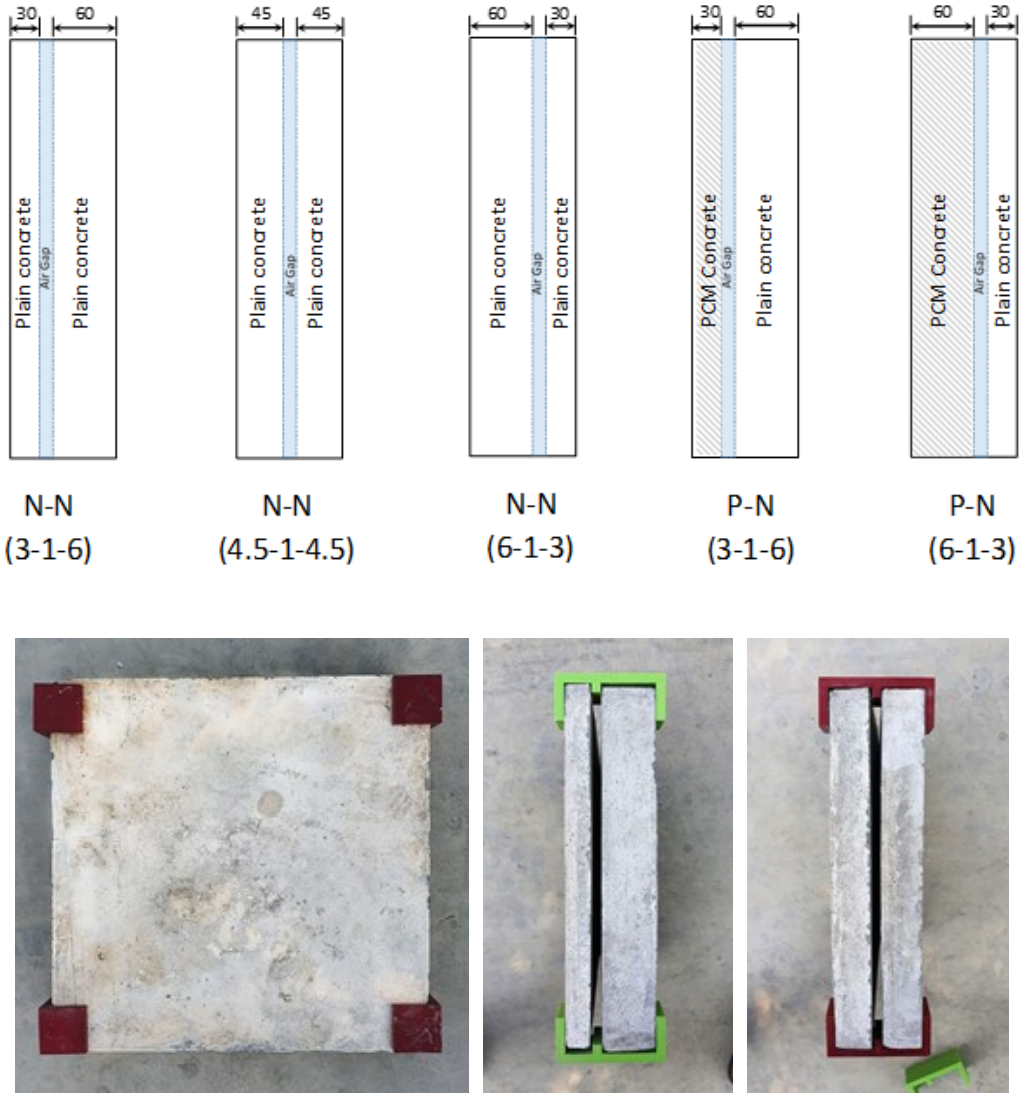

Fig. 1 Location of air gap in sandwich panels and actual pictures of specimens

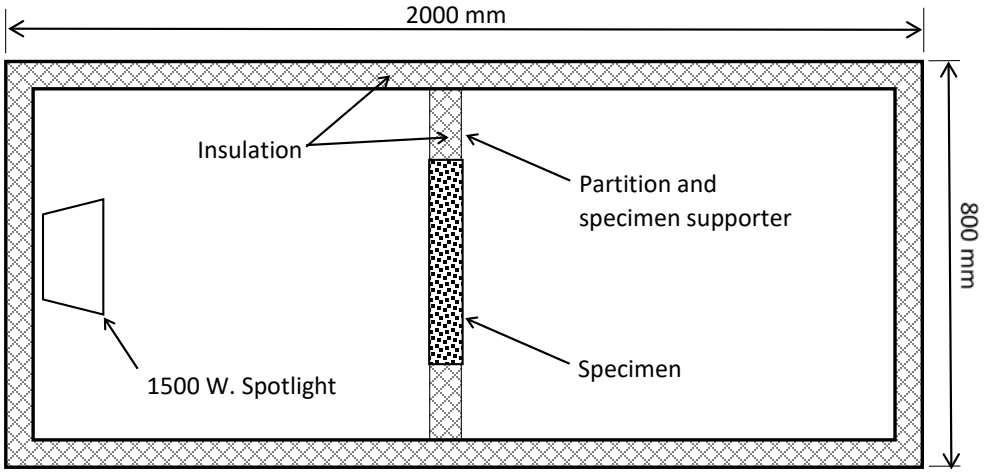

Fig.2 Thermal chamber

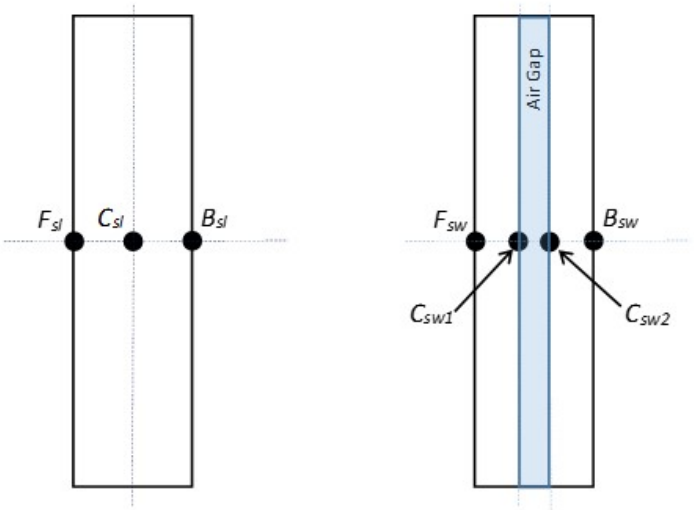

(a) (b)

Fig. 3 Thermocouple location on (a) solid and (b) sandwich panel

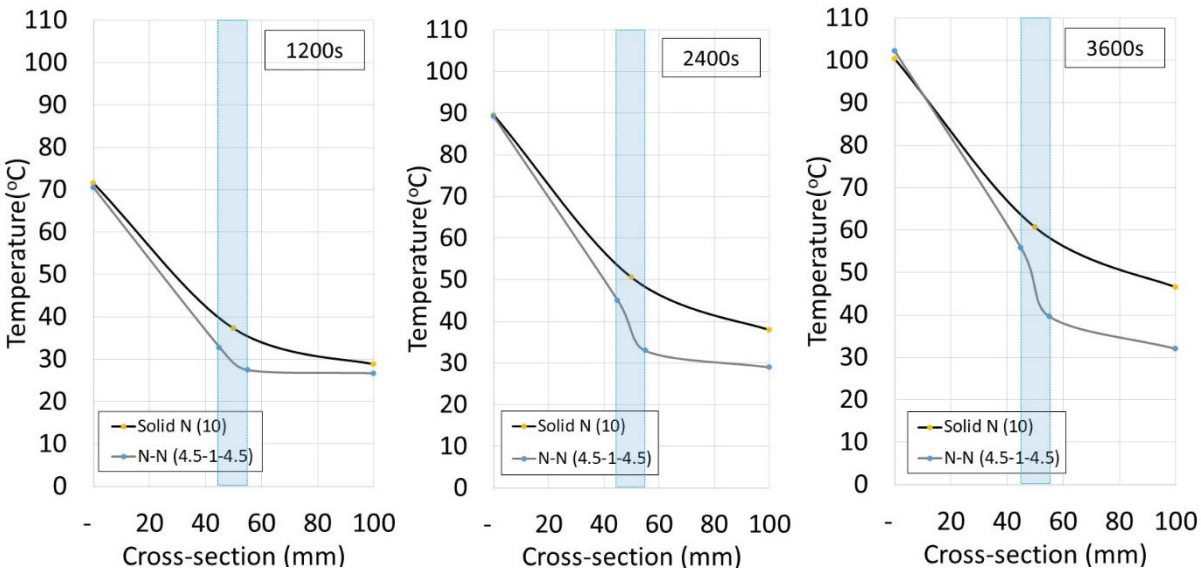

(a) 1200s (b) 2400s (c) 3600s

Fig. 4 Thermal behavior of solid and sandwich panels on heating process

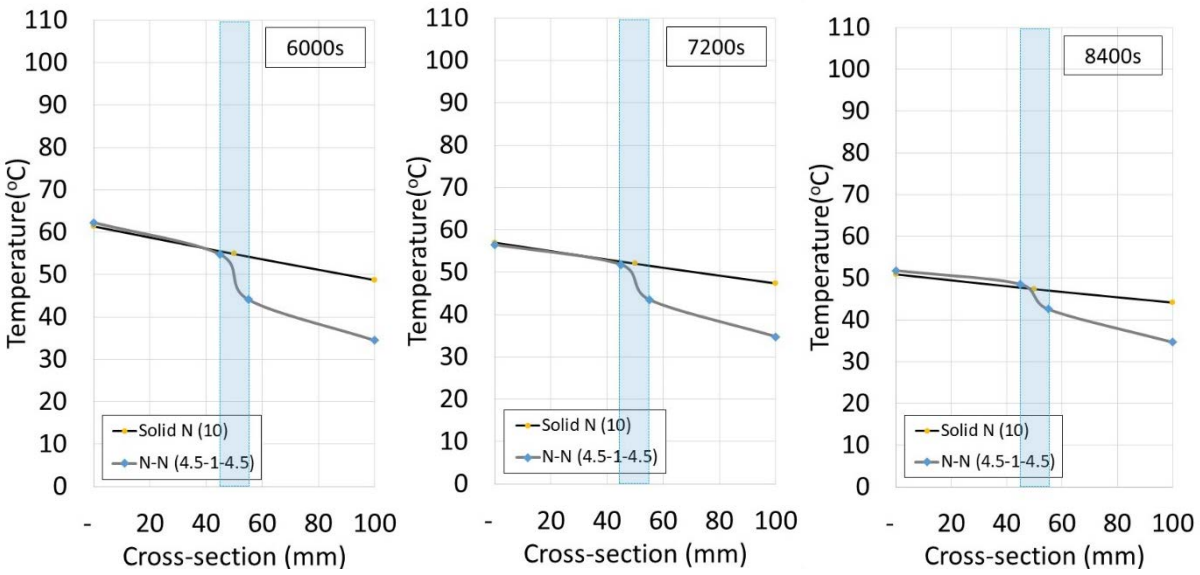

(a) 6000s (b) 7200s (c) 8400s

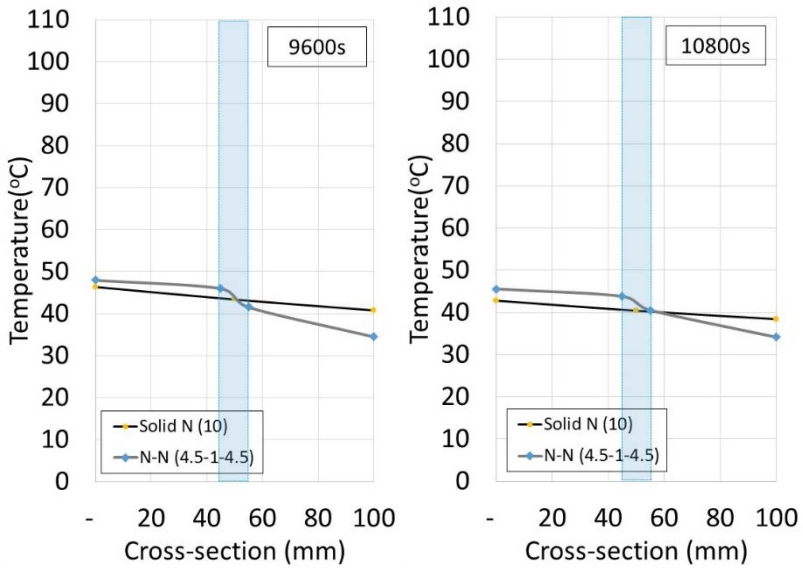

(d) 9600s (e) 10800s

Fig. 5 Thermal behavior of solid and sandwich panels on cooling cycle

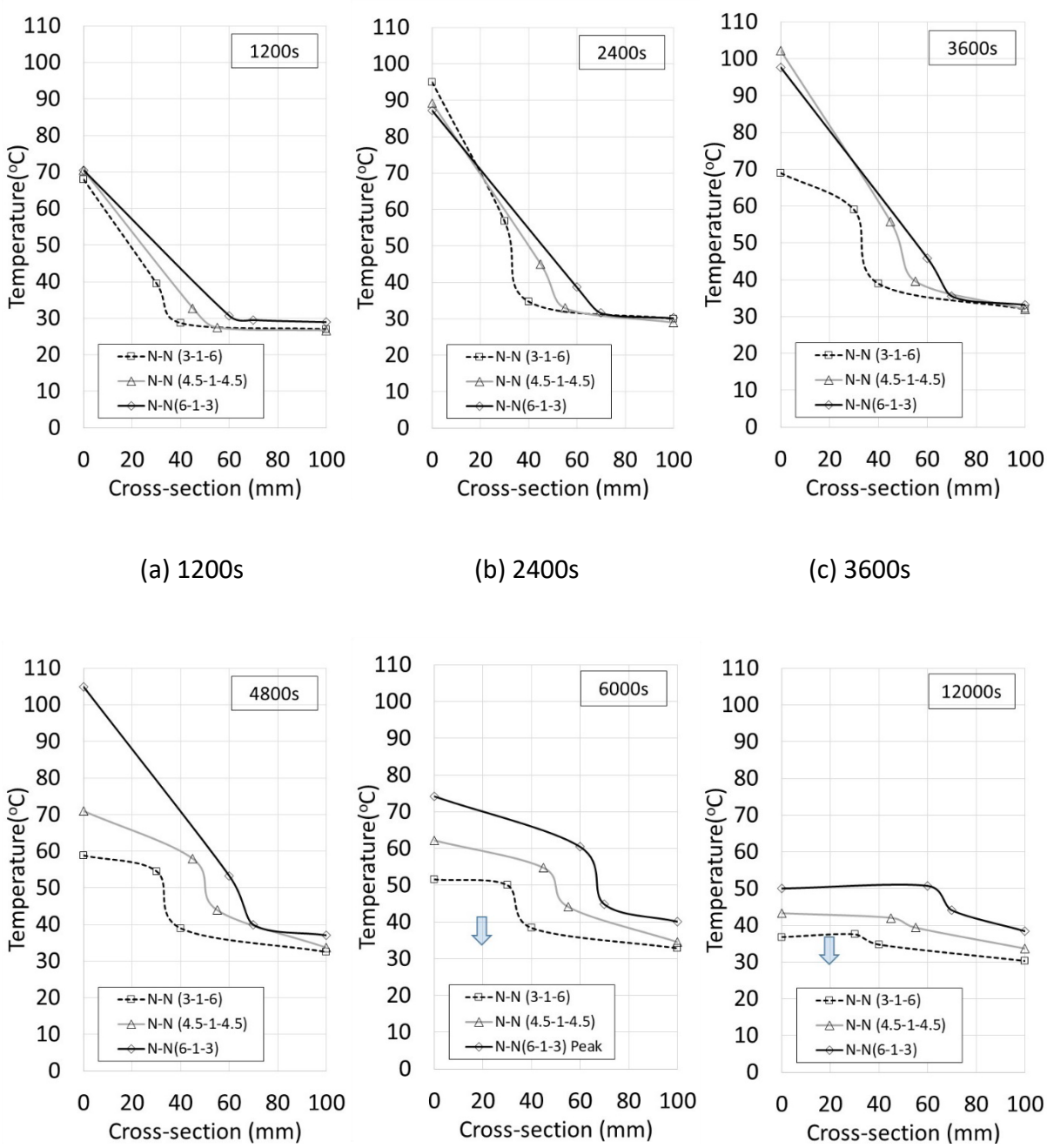

(a) 1200s (b) 2400s (c) 3600s

(d) 4800s (e) 6000s (f) 12000s

Fig. 6 Effect of air gap location on thermal behavior of sandwich panel

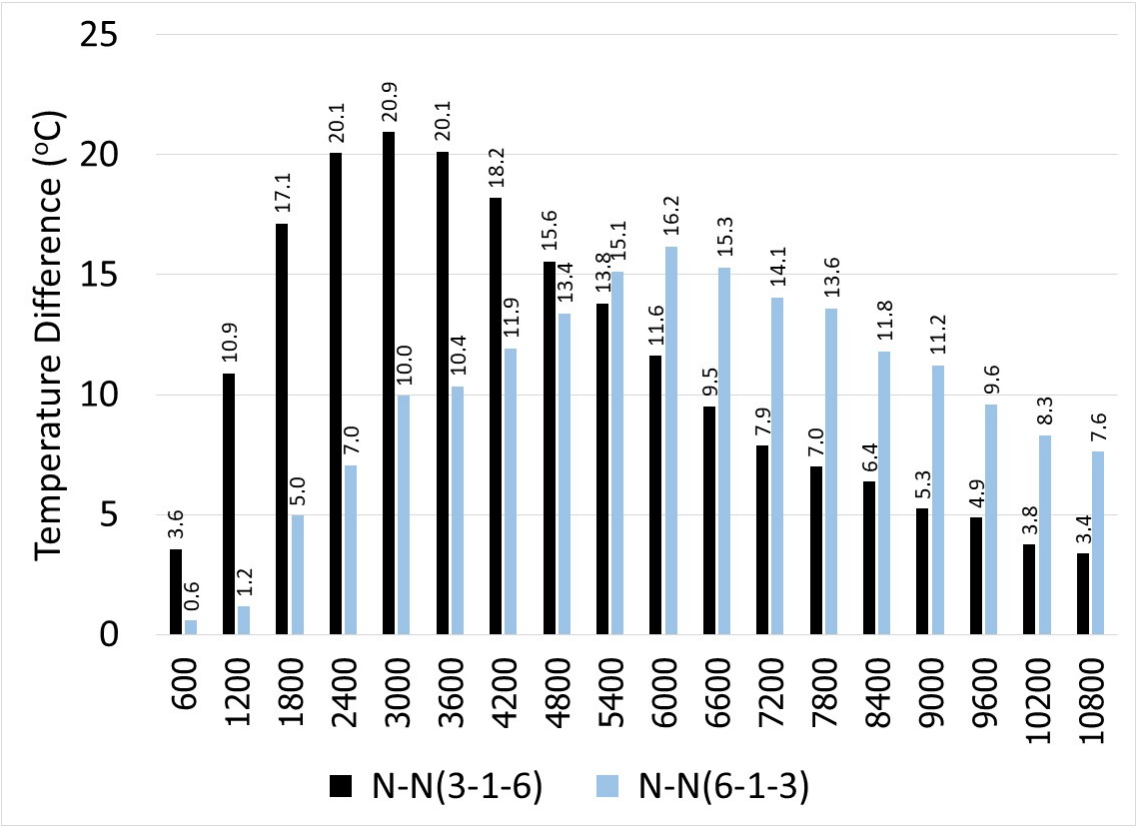

Fig. 7 Effect of air gap location on temperature lagging

time	Panel type	
	3-1-6	6-1-3
600	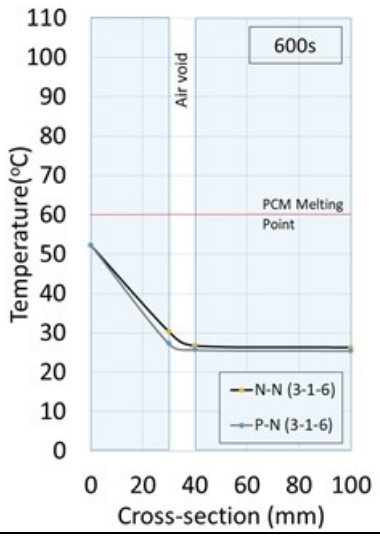	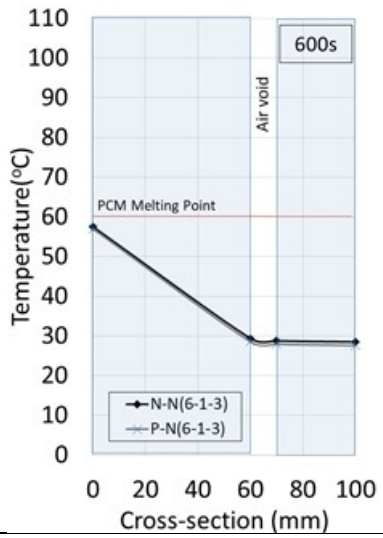
1200	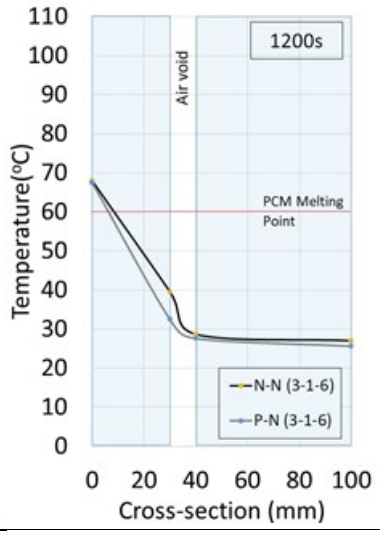	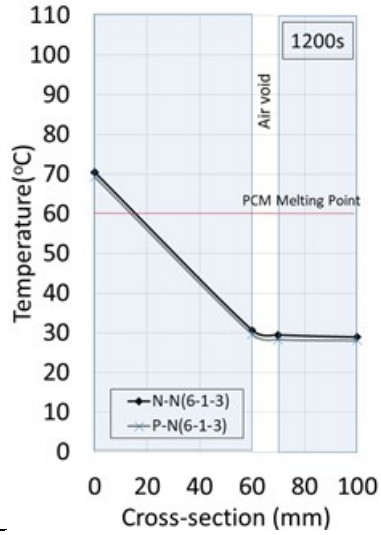
2400	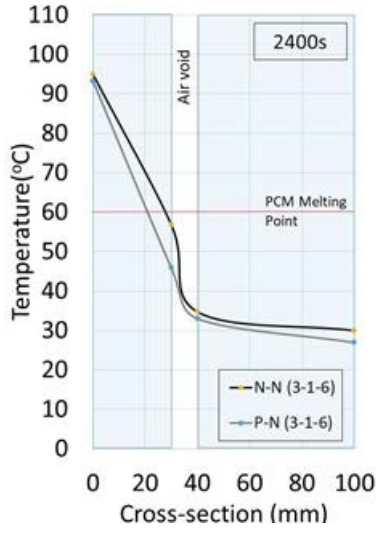	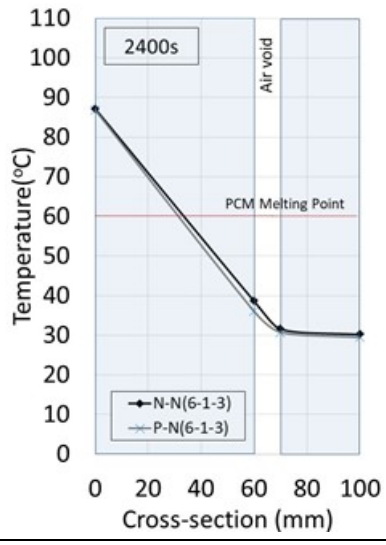

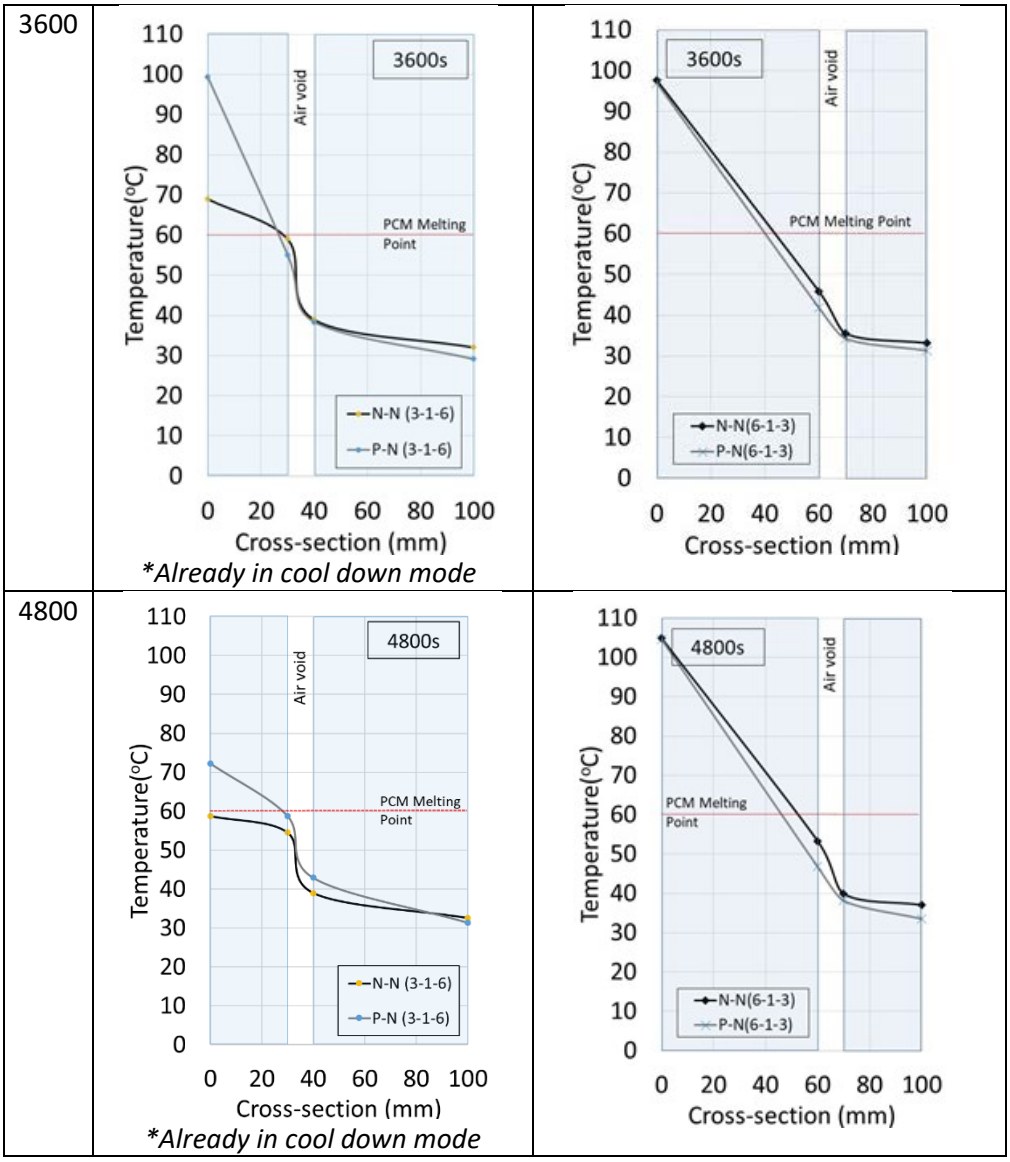

Fig. 8 Temperature movement during heat up cycle of N-N and P-N sandwich panels

time	Panel type	
	3-1-6	6-1-3
7200	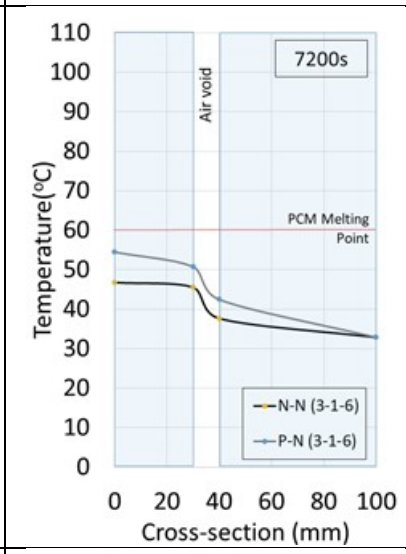	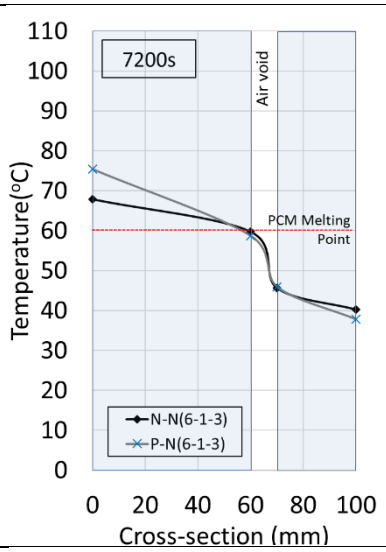
8400	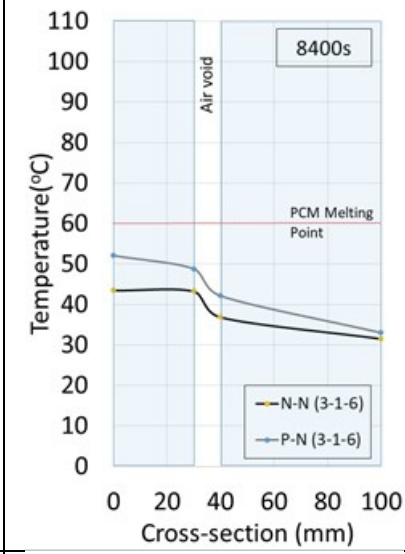	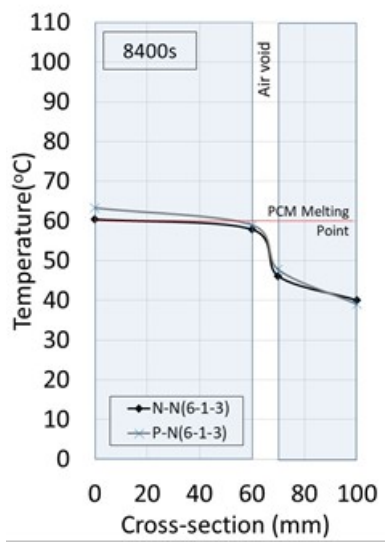
9600	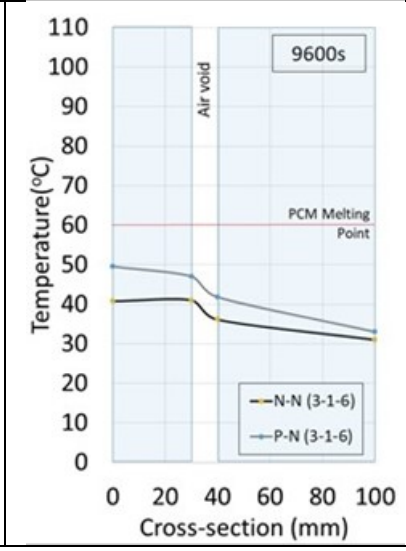	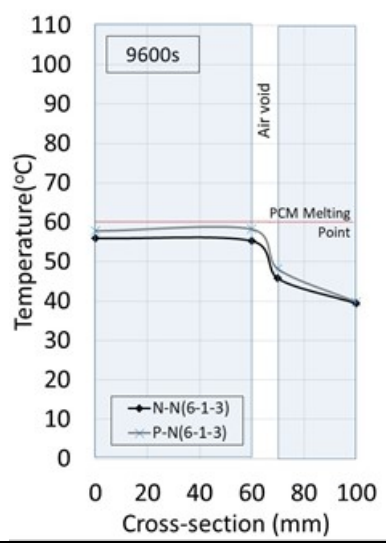

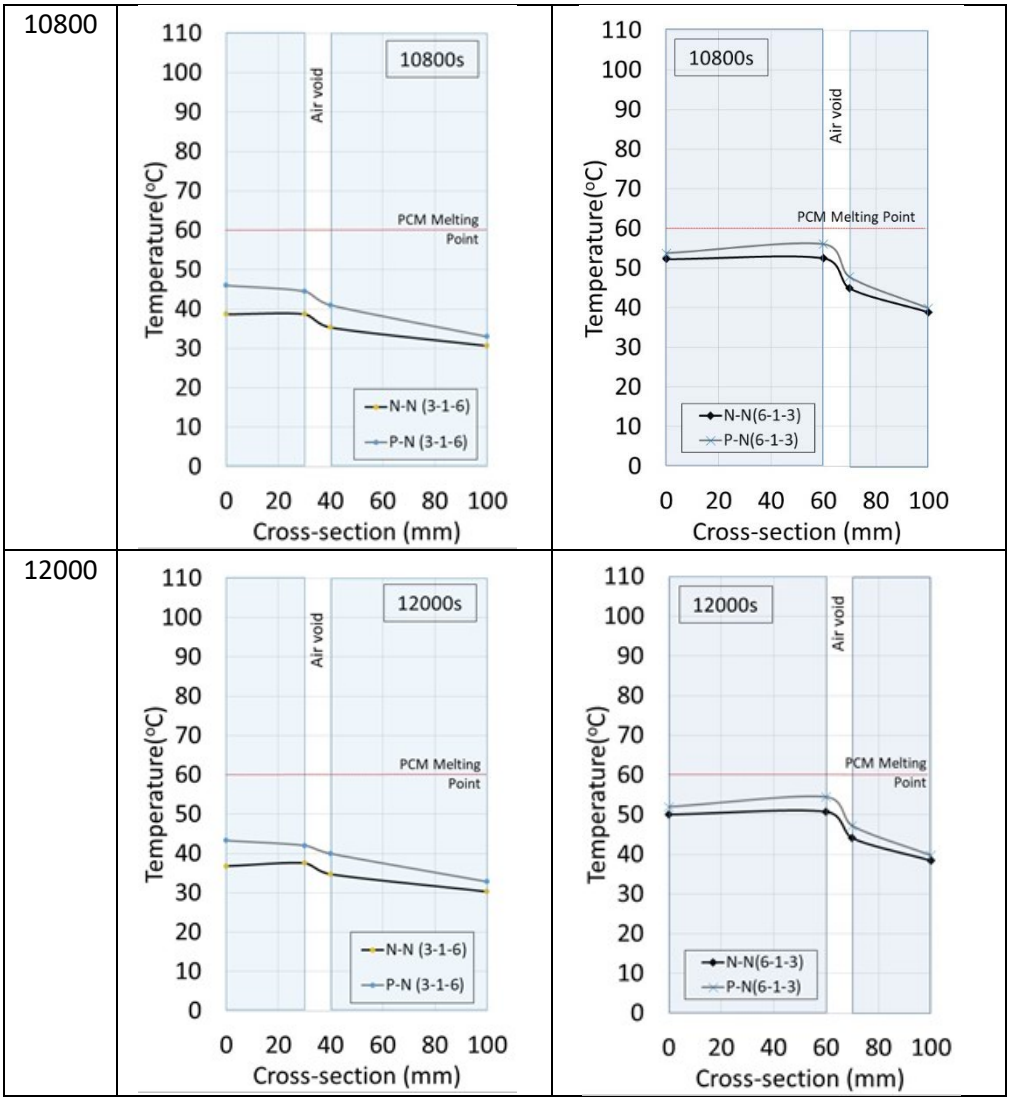

Fig. 9 Temperature movement during cool down cycle of N-N and P-N sandwich panels

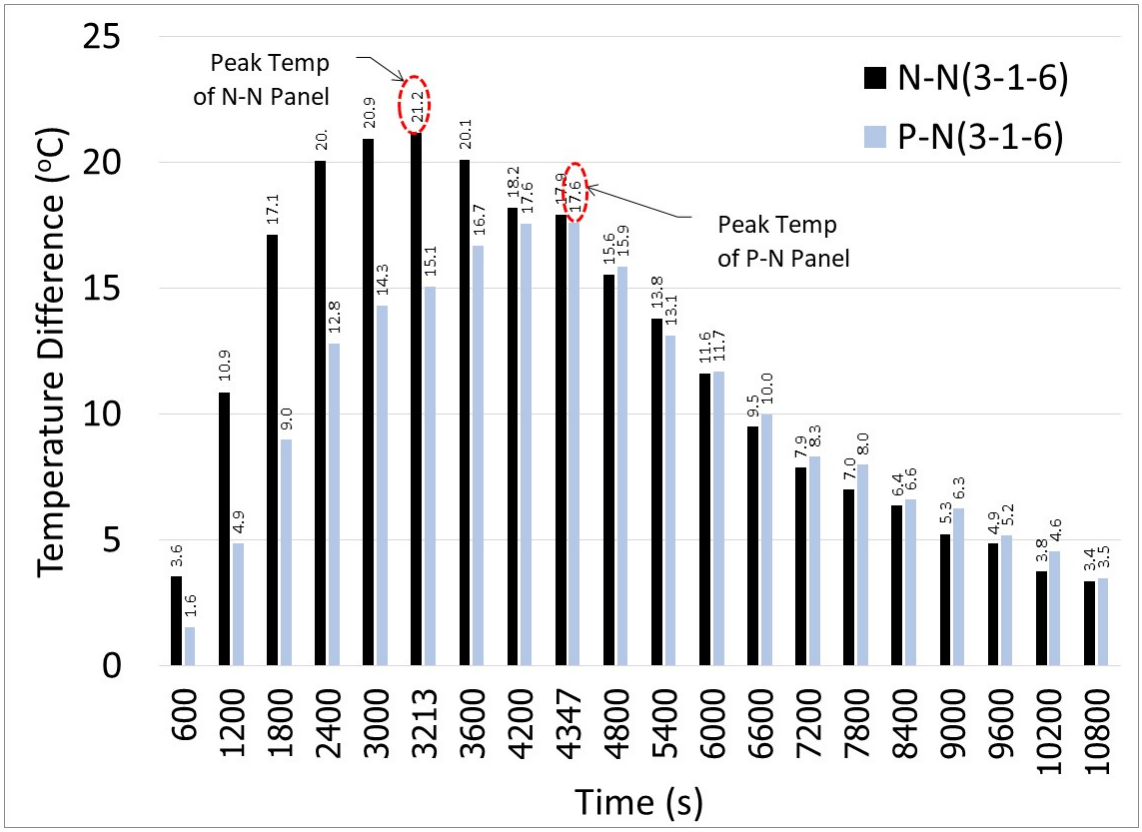

Fig. 10 Temperature lag vs Time on N-N (3-1-6) and P-N (3-1-6) panels

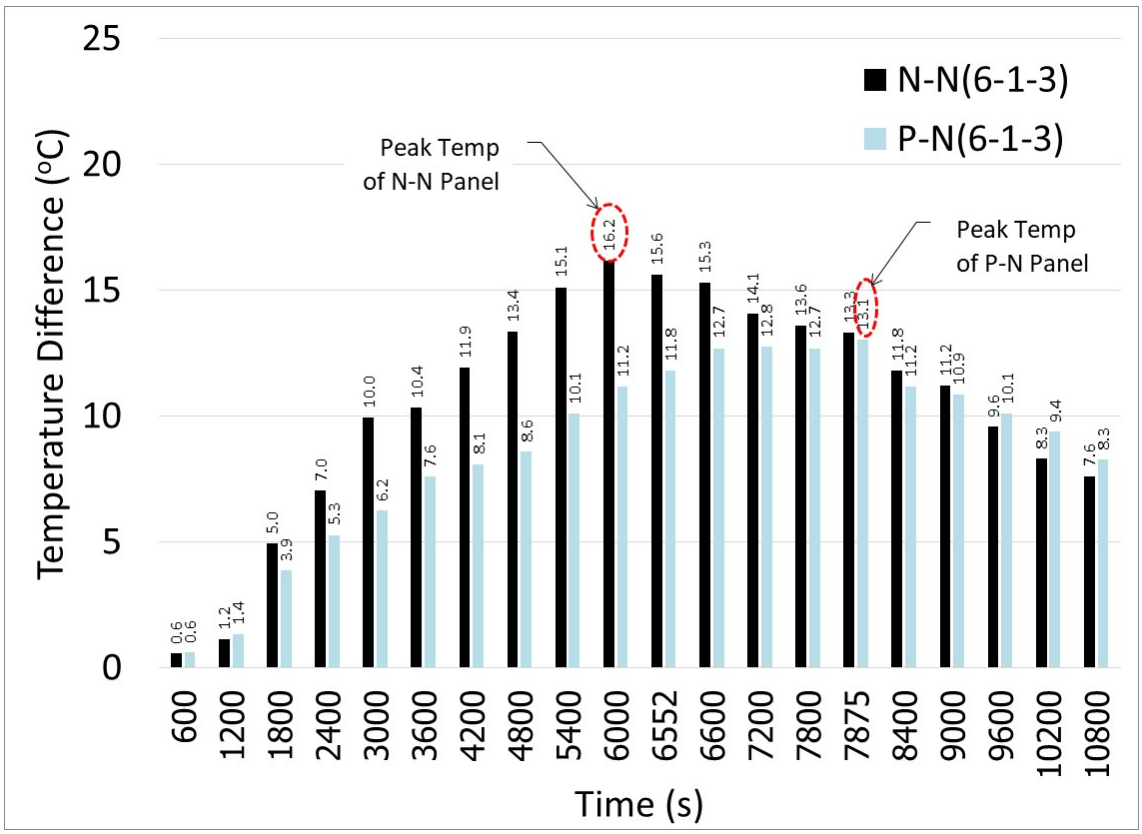

Fig. 11 Temperature lag vs Time on N-N (6-1-3) and P-N (6-1-3) panels

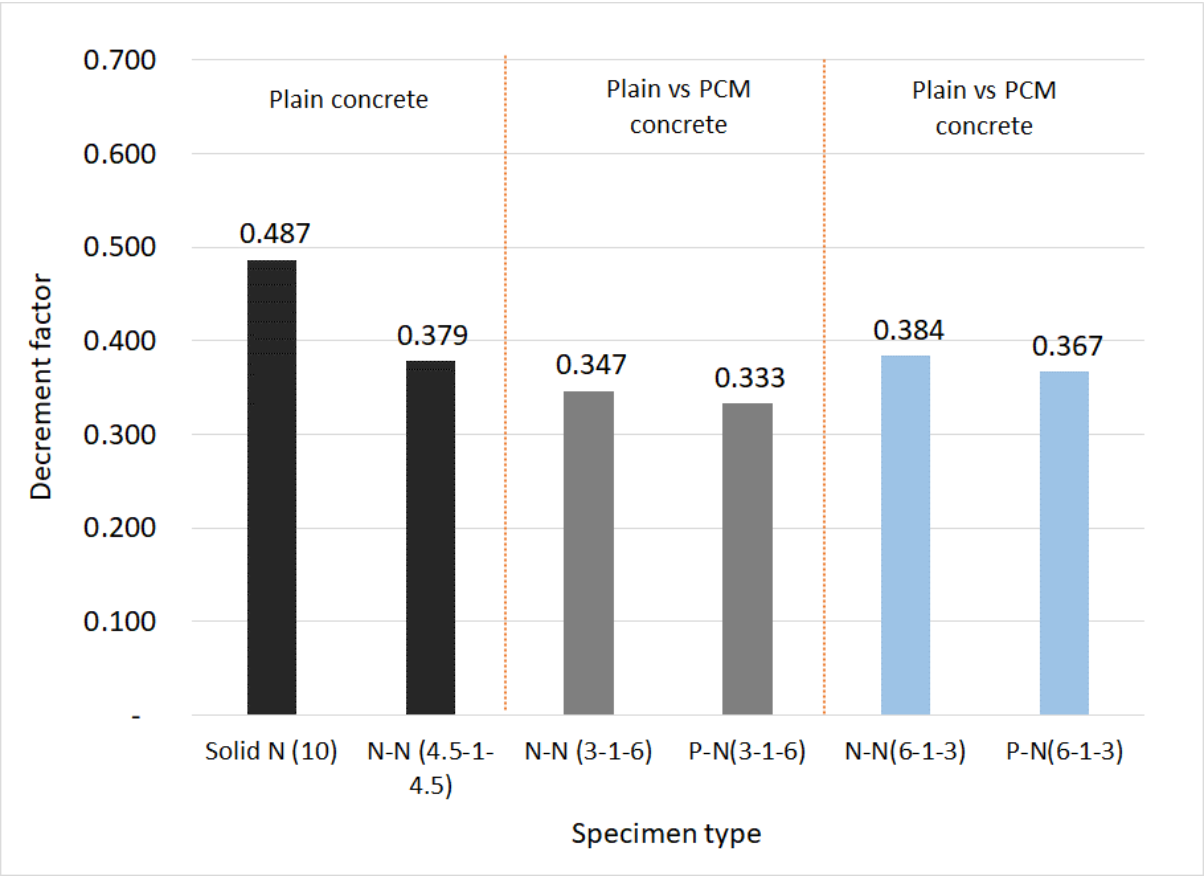

Fig. 12 Decrement factor

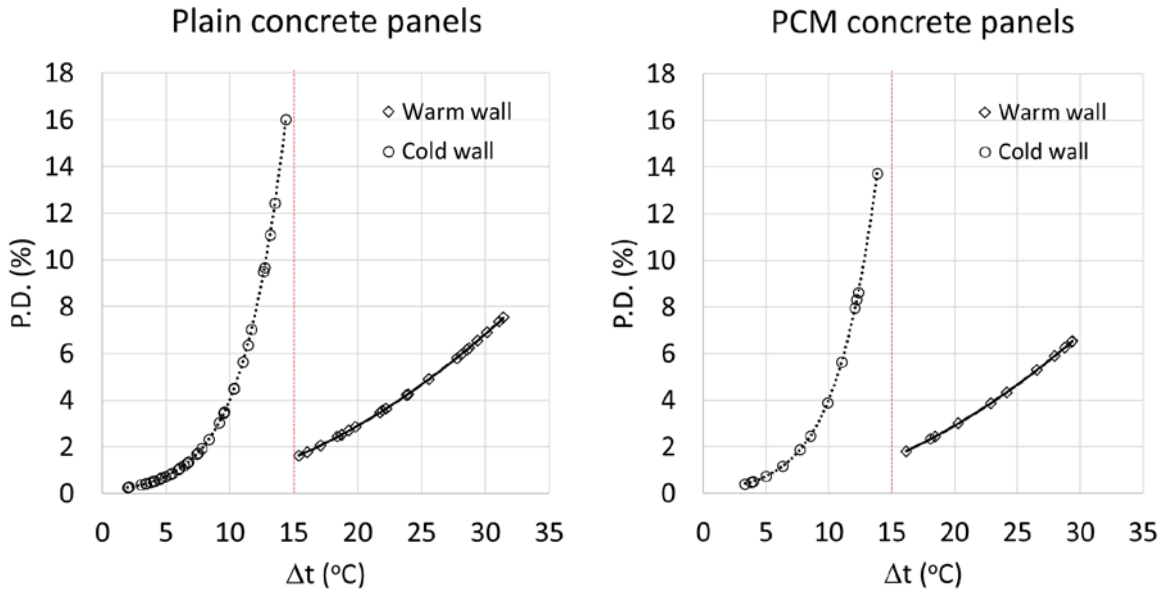

Fig. 13 Percentage dissatisfy